

Infrared Spectroscopic Characterization of the Symmetrical Hydration Motif in the $\text{SO}_2^- \cdot \text{H}_2\text{O}$ Complex

Erica A. Woronowicz, William H. Robertson, Gary H. Weddle, and Mark A. Johnson*

Sterling Chemistry Laboratory, Yale University, P.O. Box 208107, New Haven, Connecticut 06520

Evgeniy M. Myshakin and Kenneth D. Jordan*

Department of Chemistry and Center for Molecular and Materials Simulations, University of Pittsburgh, Pittsburgh, Pennsylvania 15260

Received: May 3, 2002; In Final Form: June 10, 2002

We report for the first time the vibrational spectrum of a molecular anion–water complex in which the water molecule adopts a symmetrical binding motif. In the specific complex considered, $\text{SO}_2^- \cdot \text{H}_2\text{O}$, each hydrogen atom is attached to one of the oxygen atoms of the anion. The vibrational spectrum is rather simple and is analyzed with the aid of isotopic substitution and ab initio calculations of the complex structure and harmonic vibrational frequencies. The symmetric and asymmetric OH stretching modes in the $\text{SO}_2^- \cdot \text{H}_2\text{O}$ complex are much closer in energy than in the isolated water molecule, an effect that is traced to the reduction in the HOH angle of the water molecule upon complexation.

I. Introduction

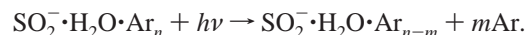
Over the past few years, vibrational predissociation spectroscopy^{1,2} has proven to be a powerful means with which to study how water binds to atomic anions.^{3–8} In all cases reported thus far, the water molecule adopts the predicted^{9–14} asymmetric configuration in which one hydrogen is attached to the ion in a so-called single ionic H-bond (SIHB) while the other hydrogen is free. With increasingly larger halides, however, the barrier in the double minimum potential decreases such that, in the $\text{I}^- \cdot \text{H}_2\text{O}$ complex, it is calculated to be on the same order as the vibrational energy of the wagging mode.³ Molecular anions provide a natural way to explore the hydration of even more extended excess charge distributions, and the vibrational spectra of the $\text{O}_2^- \cdot \text{H}_2\text{O}$ and $\text{NO}^- \cdot \text{H}_2\text{O}$ complexes have been recently reported.^{15,16} The asymmetric binding motif is again immediately evident in these molecular hydrates by the characteristic pattern of bands in the OH stretching region. In the SIHB configuration, the two OH oscillators are decoupled such that excitation of the ion-bound OH stretch dominates the spectrum and is both broad and red-shifted by hundreds of wavenumbers relative to the bands in the bare water molecule. The telltale feature of the SIHB motif, however, is the appearance of a very sharp but weak band arising from excitation of the free OH stretch that falls close to the mean of the two unperturbed stretching fundamentals around 3700 cm^{-1} .

The present paper addresses the attachment of a water molecule to the even more charge-delocalized SO_2^- ion, where the 2.6 Å distance between the two oxygen atoms in the anion is significantly larger than the (1.4 Å) separation between the hydrogen atoms in H_2O . This system was chosen since a symmetrical binding motif has already been invoked in hydration of the sulfate ion,¹⁷ for example, as well as in calculations of the binding of a water molecule to the carbonyl sulfide¹⁸ and ozonide anions.¹⁹ Here we establish some general spectroscopic features of this binding arrangement through a combined

theoretical and experimental study of the first vibrational spectra obtained for the $\text{SO}_2^- \cdot \text{H}_2\text{O}$, $\text{SO}_2^- \cdot \text{D}_2\text{O}$, and $\text{SO}_2^- \cdot \text{HDO}$ complexes.

II. Experimental Section

Vibrational spectra in the OH stretching region were obtained via argon atom predissociation spectroscopy of the $\text{SO}_2^- \cdot \text{H}_2\text{O} \cdot \text{Ar}_n$ complexes:



The presence of the Ar atoms ensures that the clusters are cold.²⁰ Spectra were recorded with differing numbers of attached argon atoms (typically $n = 1$ and 3) to ensure that our conclusions are not dependent on the extent of argon “solvation”. Size selection was achieved using the Yale tandem time-of-flight photofragmentation spectrometer, which features an ion bunching strategy to match the duty cycle of the ion source with broadly tunable pulsed lasers.²¹ The $\text{SO}_2^- \cdot \text{H}_2\text{O} \cdot \text{Ar}_n$ cluster ions were prepared with a pulsed supersonic entrainment reactor²² in which a pure argon expansion was ionized by a counter-propagating electron beam, while SO_2 and water vapor were introduced on the low pressure side of the expansion with independently controlled pulsed valves. Tunable mid-IR radiation was generated using a KTP/KTA-based optical parametric oscillator (Laser Vision), which converts the 1.5 micron idler beam from a 532 nm pumped OPO into the 3 micron region by parametric amplification with the Nd:YAG fundamental. The reported spectra are normalized for variations in the laser pulse energy over the scan.

III. Results and Discussion

The measured vibrational spectra of the $\text{SO}_2^- \cdot \text{H}_2\text{O} \cdot \text{Ar}_3$, $\text{SO}_2^- \cdot \text{HDO} \cdot \text{Ar}_3$, and $\text{SO}_2^- \cdot \text{D}_2\text{O} \cdot \text{Ar}_3$ complexes are displayed on the left side of Figure 1. A summary of the band locations is

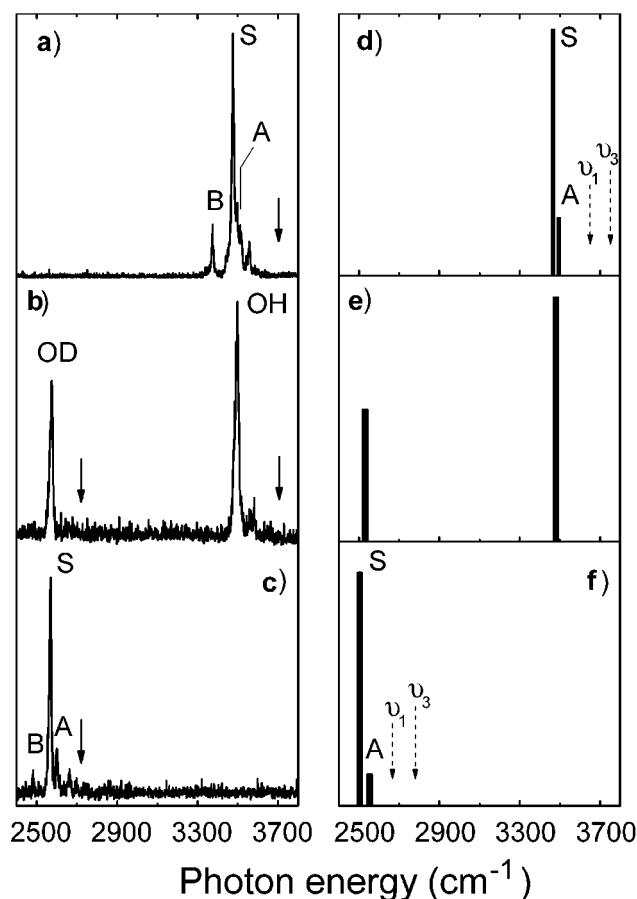


Figure 1. (Left) Vibrational predissociation spectra for (a) $\text{SO}_2^- \cdot \text{H}_2\text{O} \cdot \text{Ar}_3$, (b) $\text{SO}_2^- \cdot \text{HDO} \cdot \text{Ar}_3$, and (c) $\text{SO}_2^- \cdot \text{D}_2\text{O} \cdot \text{Ar}_3$, recorded by observing loss of three argon atoms. (Right) Ab initio calculations (corrected for anharmonicity) of (d) $\text{SO}_2^- \cdot \text{H}_2\text{O}$, (e) $\text{SO}_2^- \cdot \text{HDO}$, and (f) $\text{SO}_2^- \cdot \text{D}_2\text{O}$. Dotted arrows indicate the symmetric and asymmetric stretches for an isolated water molecule. Solid arrows indicate the centroid of the isolated water stretches, corresponding to the frequencies of free OH (OD) stretch. Labels correspond to S = symmetric OH (OD) stretch, A = asymmetric OH (OD) stretch, B = HOH (DOD) bend overtone ($2\nu_2$), while OH and OD denote uncoupled stretches in HDO.

TABLE 1: Calculated^a and Observed Frequencies (cm^{-1}) for SO_2^- Monohydrates

mode	H_2O		D_2O		HDO	
	calc	obs	calc	obs	calc	obs
asymmetric stretch	3494	3515	2554	2600	3479 ^b	3500 ^b
symmetric stretch	3466	3475	2503	2570	2530 ^c	2575 ^c
HOH bend	1618	1688 ^d	1184	1240 ^d	1421	
($\text{H}_2\text{O}-\text{O}$) ₂ stretch	177		171		173	
$\text{H}_2\text{O}+\text{SO}_2$ rock	113	85	109	90	110	85
SO_2 wag	47		47		47	

^a Scaled by 0.95 to account for anharmonicity, chosen to normalize the calculated harmonic asymmetric stretching quantum to the observed transition energy in bare H_2O . ^b Isolated OH stretch. ^c Isolated OD stretch. ^d $1/2(2\nu_2)$.

presented in Table 1, along with the theoretical predictions and band assignments. The spectra of the $\text{SO}_2^- \cdot \text{H}_2\text{O}$ and $\text{SO}_2^- \cdot \text{D}_2\text{O}$ isotopomers are simple and dominated by a single strong transition, which in each case occurs significantly below the energies of the hydrogenic stretches in free water (dotted arrows in Figure 1).²³ This red-shift is larger in the H_2O complex (232 cm^{-1}) than in the D_2O complex (159 cm^{-1}). The $\text{SO}_2^- \cdot \text{HDO}$ spectrum displays two sharp bands, one each in the OH and

OD stretching regions. Particularly noteworthy in this case is the absence of transitions in the vicinity of either free OH or OD stretch vibrations (solid arrows in Figure 1), immediately suggesting a double-donor binding motif.

There are several weaker bands on either side of the intense peaks in the $\text{SO}_2^- \cdot \text{H}_2\text{O}$ and $\text{SO}_2^- \cdot \text{D}_2\text{O}$ spectra as well as on the high-frequency side of the intense OH transition in the $\text{SO}_2^- \cdot \text{HDO}$ spectrum. Candidates for these extra bands include combination bands involving soft modes associated with the relative motion of the water molecule against the ion and, in the case of H_2O or D_2O , a second OH (or OD) stretch fundamental in addition to overtones of the intramolecular bending mode (ν_2) in the H_2O moiety.

Based on comparison of the spectra for the three isotopomers, we conclude that the intense lines near 3500 cm^{-1} in $\text{SO}_2^- \cdot \text{H}_2\text{O}$ and $\text{SO}_2^- \cdot \text{HDO}$ are due to an OH stretch fundamental transition and those near 2575 cm^{-1} in the spectra of $\text{SO}_2^- \cdot \text{HDO}$ and $\text{SO}_2^- \cdot \text{D}_2\text{O}$ are due to an OD stretch fundamental. The isotopic substitution study also shows that the weak lines at 3375 cm^{-1} in $\text{SO}_2^- \cdot \text{H}_2\text{O}$ and 2480 cm^{-1} $\text{SO}_2^- \cdot \text{D}_2\text{O}$ are due to the (020) overtone of the intramolecular bending vibration and are labeled B in Figure 1. Note that this assignment places the $\nu=2$ level of the HOH bend appreciably higher in energy than that found in the asymmetrically bonded anion–water complexes ($3200\text{--}3300 \text{ cm}^{-1}$). The keys to this assignment are the absence of corresponding lines in the IR spectrum of $\text{SO}_2^- \cdot \text{HDO}$ and the relative intensity of the band in the $\text{SO}_2^- \cdot \text{H}_2\text{O}$ spectrum. The nominally forbidden bend overtone usually appears in the spectra of anion–water complexes via intensity borrowing from the OH stretching transition, which is mediated by a Fermi-resonance interaction. Since the matrix element for this interaction is typically close to 33 cm^{-1} ,^{5,7} the band disappears in the HOD modification since the bend overtone becomes well separated from the OH (or OD) stretch $\nu=1$ level (see Table 1). In $\text{SO}_2^- \cdot \text{H}_2\text{O}$, the observed intensity of the 3375 cm^{-1} feature relative to that of the main band (0.135) requires a Fermi interaction matrix element of 32.4 cm^{-1} , in excellent agreement with the value found in the halide hydrates. The fact that the bending overtone associated with the $\text{SO}_2^- \cdot \text{D}_2\text{O}$ complex (at 2480 cm^{-1}) is much weaker than this transition in the H_2O species would seem to reflect a substantially weaker matrix element for the interaction with the increase in mass.

The strong OH and OD stretch fundamentals of $\text{SO}_2^- \cdot \text{H}_2\text{O}$ and $\text{SO}_2^- \cdot \text{D}_2\text{O}$ are accompanied by two weak peaks approximately 40 and 85 cm^{-1} higher in energy. In contrast, the intense OH stretch fundamental in $\text{SO}_2^- \cdot \text{HDO}$ appears with only the 85 cm^{-1} companion to the blue. The absence of the $\sim 40 \text{ cm}^{-1}$ peak in the $\text{SO}_2^- \cdot \text{HDO}$ spectrum leads us to conclude that this feature corresponds to the second OH (or OD) stretch fundamental in the $\text{SO}_2^- \cdot \text{H}_2\text{O}$ and $\text{SO}_2^- \cdot \text{D}_2\text{O}$ complexes. This band is particularly clear in the $\text{SO}_2^- \cdot \text{D}_2\text{O}$ spectrum as the high energy shoulder is more congested in the case of $\text{SO}_2^- \cdot \text{H}_2\text{O}$. While this assignment indicates that there is an unusually small splitting between the symmetric and asymmetric modes (i.e., compared to the 100 cm^{-1} spacing in bare H_2O), it is nonetheless supported by the evolution of the bands with isotopic substitution. The strong OH and OD stretch bands are slightly blue shifted in the spectrum of the $\text{SO}_2^- \cdot \text{HDO}$ isotopomer as compared to the spectra of $\text{SO}_2^- \cdot \text{H}_2\text{O}$ and $\text{SO}_2^- \cdot \text{D}_2\text{O}$. This result would be expected if the decoupled (OH and OD) oscillators adopt energies close to the centroid of the ν_1 and ν_3 transitions in the homogeneous isotopomers. This blue shift is, in fact, opposite to that anticipated upon removal of

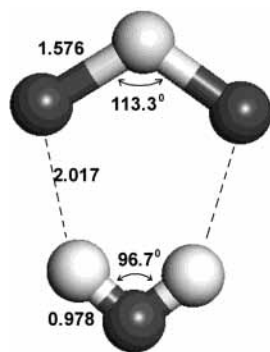


Figure 2. Ab initio structure of $\text{SO}_2 \cdot \text{H}_2\text{O}$ calculated at the MP2/aug-cc-pVDZ^{24–26} level. The complex adopts a symmetrical (C_{2v}) binding motif.

the Fermi resonance interaction with the bend, which acts to raise the energy of the symmetric stretch (by about 10 cm^{-1} in $\text{SO}_2 \cdot \text{H}_2\text{O}$). Note that the close proximity of the symmetric and asymmetric OH stretching bands immediately explains why the frequency of the dominant band is relatively insensitive to substitution of one of the H atoms by D. Having assigned the closest feature to an OH stretching mode, we are left with the second weak feature which appears about 85 cm^{-1} to the blue of the intense lines in all three isotopomers. Because of this insensitivity to H/D substitution, this band is attributed to a combination band involving a soft mode of the cluster.⁵

While we can deduce many assignments of the bands based on direct analysis of the spectra, it is not possible to establish on this basis alone whether the dominant bands are due to the symmetric or asymmetric OH (OD) stretching modes. Nor is it obvious why the coupled oscillators display a much narrower separation in the complex than in isolated water molecules. To clarify these issues, we turn to ab initio electronic structure calculations of the $\text{SO}_2 \cdot \text{H}_2\text{O}$ cluster geometry and harmonic vibrational frequencies. The calculations, carried out at the MP2/aug-cc-pVDZ^{24–26} level of theory recover the C_{2v} symmetry double-donor structure displayed in Figure 2. All calculated vibrational frequencies are positive, confirming that this structure is indeed a minimum on the potential energy surface. Both the OSO angle of the SO_2 molecule and the HOH angle of the water molecule decrease as a result of the complexation, with the bond angle in water contracting by about 7° and that in the SO_2 only about 1° .

Table 1 lists the calculated frequencies, scaled by a factor of 0.95 to correct approximately for anharmonicity effects, together with our assignments of the experimentally observed transitions. There is generally good agreement between the calculated and observed spectra for all three isotopomers. For the $\text{SO}_2 \cdot \text{HDO}$ system, the calculations predict the OH and OD vibrations to occur at 3479 and 2530 cm^{-1} , which are just below the measured frequencies of the intense modes (by 21 and 45 cm^{-1} , respectively) as indicated in Table 1. In the H_2O and D_2O variations, the symmetric (ν_1) OH stretch fundamental is calculated to be much more intense than the asymmetric (ν_3) OH stretch, and the 28 cm^{-1} predicted spacing between the modes in $\text{SO}_2 \cdot \text{H}_2\text{O}$ is indeed much closer than the 100 cm^{-1} splitting found in the isolated water molecule.²³ This leads us to assign the dominant bands in the $\text{SO}_2 \cdot \text{H}_2\text{O}$ and $\text{SO}_2 \cdot \text{D}_2\text{O}$ spectra to the symmetric stretching fundamentals and supports our assignment of the associated asymmetric stretching fundamentals to weak bands which are unusually close in energy.

The reduction in the splitting between the ν_1 and ν_3 OH stretching modes in the $\text{SO}_2 \cdot \text{H}_2\text{O}$ complex is an important

observation and warrants further discussion. Sadlej et al. have reported a similar conclusion in their analysis of the larger $[(\text{H}_2\text{O})_{8–10}]$ neutral cluster systems, where they assign the observed $\sim 25–30 \text{ cm}^{-1}$ doublet near 3500 cm^{-1} to ν_1 and ν_3 transitions of water molecules in double donor–acceptor (DDA) H-bonding environments.²⁷ These authors note that such a collapse in the splitting must reflect changes in the momentum and potential coupling between the OH oscillators, but do not recover the magnitude of the effect in their ab initio calculations (e.g., calculated splitting of 90 cm^{-1} vs an experimental value of $24–30 \text{ cm}^{-1}$) or discuss its mechanical cause. To explore the physical origin of the effect in the $\text{SO}_2 \cdot \text{H}_2\text{O}$ case, we calculated the normal mode eigenvalues for a hypothetical H–O–H system with fixed force constants appropriate for an isolated water molecule but with variable G-matrix elements associated with an arbitrary H–O–H bond angle. (Note that the G matrix is diagonal at 90° .) Diagonalization of this FG matrix²⁸ indicates that the ν_1 and ν_3 energies intersect at an HOH angle of about 78° and reverse order upon further reduction of the bond angle. At the angle of intersection, the coupling between the oscillators vanishes and the two modes of differing symmetry become degenerate. Since a major distortion of the water molecule upon formation of the complex is the reduction in HOH bond angle from 104° to 96.7° , it seems that this geometrical change causes partial decoupling of the modes with a concomitant reduction in the splitting in the OH stretching modes.

One puzzling aspect of this complex's behavior is the high frequency of the bending overtone, which appears about 125 cm^{-1} above its typical location in asymmetric complexes.^{5,7} The calculations give an HOH bending frequency of 1618 cm^{-1} , which would place the overtone near 3236 cm^{-1} as would be expected, but considerably below the observed 3375 cm^{-1} feature. Two effects seem likely to account for this discrepancy. First, the vibration levels of the bending mode could display negative anharmonicity as a consequence of the symmetrical binding motif, or second, this could be a case where the extent of intermolecular charge transfer changes with HOH angle. In the latter circumstance, accurate theoretical treatment of the potential energy surface would require adoption of a multiconfigurational reference wave function.

Finally, we address the assignment of the combination band involving a soft mode of the complex with an energy of about 85 cm^{-1} . The intermolecular rock vibration, calculated to have an energy of $\sim 110 \text{ cm}^{-1}$, has the closest energy match to the observed band displacement. Interestingly, this combination band is clearly more intense in the OH region compared to the OD region, which suggests that the coupling between the high frequency stretch and the intermolecular motion is scaling with the frequency or the amplitude of the high frequency oscillator. One general consequence of the quenching both of the Fermi-resonant interaction with the bend and this coupling to soft modes is that the OD stretching region gives rise to qualitatively simpler spectra than does the spectrum of the OH stretches.

IV. Summary

The vibrational predissociation spectrum of the $\text{SO}_2 \cdot \text{H}_2\text{O} \cdot \text{Ar}_n$ ion–molecule complex does not display a free OH feature, indicating the formation of a symmetrical binding configuration involving ionic H-bonds to both hydrogen atoms. Ab initio calculations confirm that this binding motif is a minimum on the potential surface and indicate that the dominant band observed in the spectrum is due to the symmetric OH stretching fundamental with a weaker band arising from the asymmetric

stretch just above it. The close separation between the symmetric and asymmetric OH stretching vibrational levels is traced to the reduction in the HOH bond angle upon formation of the complex, which acts to reduce the kinetic coupling between the motion of the two localized OH stretch oscillators.

Acknowledgment. M.A.J. and K.J.D. acknowledge support from the National Science Foundation under grants CHE-0111245 and CHE-0078528, respectively. We also acknowledge helpful discussions with Prof. D. J. Nesbitt regarding the coupling of the stretching modes in H₂O.

References and Notes

- (1) Duncan, M. A. *Int. J. Mass. Spectrom.* **2000**, *200*, 545–569.
- (2) Bieske, E. J.; Dopfer, O. *Chem. Rev.* **2000**, *100*, 3963–3998.
- (3) Johnson, M. S.; Kuwata, K. T.; Wong, C.-K.; Okumura, M. *Chem. Phys. Lett.* **1996**, *260*, 551–557.
- (4) Bailey, C. G.; Kim, J.; Dessent, C. E. H.; Johnson, M. A. *Chem. Phys. Lett.* **1997**, *269*, 122–127.
- (5) Ayotte, P.; Weddle, G. H.; Kim, J.; Johnson, M. A. *J. Am. Chem. Soc.* **1998**, *120*, 12361–12362.
- (6) Ayotte, P.; Kelley, J. A.; Nielsen, S. B.; Johnson, M. A. *Chem. Phys. Lett.* **2000**, *316*, 455–459.
- (7) Robertson, W. H.; Weddle, G. H.; Kelley, J. A.; Johnson, M. A. *J. Phys. Chem. A* **2002**, *106*, 1205–1209.
- (8) Cabarcos, O. M.; Weinheimer, C. J.; Xantheas, S. S.; Lisy, J. M. *J. Chem. Phys.* **1999**, *110*, 5–8.
- (9) Irle, S.; Bowman, J. M. *J. Chem. Phys.* **2000**, *113*, 8401–8403.
- (10) Xantheas, S. S. *J. Phys. Chem.* **1996**, *100*, 9703–9713.
- (11) Thompson, W. H.; Hynes, J. T. *J. Am. Chem. Soc.* **2000**, *122*, 6278–6286.
- (12) Kim, J.; Lee, H. M.; Suh, S. B.; Majumdar, D.; Kim, K. S. *J. Chem. Phys.* **2000**, *113*, 5259–5272.
- (13) Zhao, X. G.; Gonzales-Lafont, A.; Truhlar, D. G.; Steckler, R. J. *Chem. Phys.* **1991**, *94*, 5544–5558.
- (14) Yates, B. F.; Schaefer, H. F., III; Lee, T. J.; Rice, J. E. *J. Am. Chem. Soc.* **1988**, *110*, 6327–6332.
- (15) Weber, J. M.; Kelley, J. A.; Robertson, W. H.; Johnson, M. A. *J. Chem. Phys.* **2001**, *114*, 2698–2706.
- (16) Robertson, W. H.; Myshakin, E. M.; Jordan, K. D.; Johnson, M. A., unpublished.
- (17) Wang, X. B.; Yang, X.; Nicholas, J. B.; Wang, L. S. *Science* **2001**, *294*, 1322–1325.
- (18) Surber, E.; Ananthavel, S. P.; Sanov, A. *J. Chem. Phys.* **2002**, *116*, 1920–1929.
- (19) Bentley, J.; Collins, Y. T.; Chipman, D. M. *J. Phys. Chem. A* **2000**, *104*, 4629–4635.
- (20) Ayotte, P.; Weddle, G. H.; Kim, J.; Johnson, M. A. *Chem. Phys.* **1998**, *239*, 485–491.
- (21) Johnson, M. A.; Lineberger, W. C. In *Techniques for the study of gas-phase ion molecule reactions*; Farrar, J. M., Saunders, J. W., Eds.; Wiley: New York, 1988; p 591.
- (22) Robertson, W. H.; Kelley, J. A.; Johnson, M. A. *Rev. Sci. Instrum.* **2000**, *71*, 4431–4433.
- (23) Shimanouchi, T. Molecular Vibrational Frequencies. In *NIST Chemistry WebBook, NIST Standard Reference Database*; Mallard, W. G., Linstrom, P. J., Eds.; National Institute of Standards and Technology (<http://webbook.nist.gov>): Gaithersburg, MD, 1998; Vol. 69.
- (24) Kendall, R. A.; Dunning, T. H., Jr.; Harrison, R. J. *J. Chem. Phys.* **1992**, *96*, 6796.
- (25) Woon, D. E.; Dunning, T. H., Jr. *J. Chem. Phys.* **1993**, *98*, 1358.
- (26) The calculations were performed using GAUSSIAN 98. Frisch, M. J.; Trucks, G. W.; Schlegel, H. B.; Scuseria, G. E.; Robb, M. A.; Cheeseman, J. R.; Zakrzewski, V. G.; Montgomery, J. A.; Stratmann, R. E.; Burant, J. C.; Dapprich, S.; Millam, J. M.; Daniels, A. D.; Kudin, K. N.; Strain, M. C.; Farkas, O.; Tomasi, J.; Barone, V.; Cossi, M.; Cammi, R.; Mennucci, B.; Pomelli, C.; Adamo, C.; Clifford, S.; Ochterski, J.; Petersson, G. A.; Ayala, P. Y.; Cui, Q.; Morokuma, K.; Malick, D. K.; Rabuck, A. D.; Raghavachari, K.; Foresman, J. B.; Cioslowski, J.; Ortiz, J. V.; Baboul, A. G.; Stefanov, B. B.; Liu, G.; Liashenko, A.; Piskorz, P.; Komaromi, I.; Gomperts, R.; Martin, R. L.; Fox, D. J.; Keith, T.; Al-Laham, M. A.; Peng, C. Y.; Nanayakkara, A.; Challacombe, M.; Gill, P. M. W.; Johnson, B.; Chen, W.; Wong, M. W.; Andres, J. L.; Gonzalez, C.; Head-Gordon, M.; Replogle, E. S.; Pople, J. A. Gaussian, Inc.: Pittsburgh, 1998.
- (27) Sadlej, J.; Buch, V.; Kazimirski, J. K.; Buck, U. *J. Phys. Chem.* **1999**, *103*, 4933.
- (28) Bernath, P. *Spectra of Atoms and Molecules*; Oxford University Press: New York, 1995; pp 227–233.